UNIVERSITY OF CALIFORNIA SAN DIEGO

High Open-Ocean Productivity in a Greenhouse World

A thesis submitted in partial satisfaction of the requirements for the degree Master of Science

in

Oceanography

by

Zev Brook

Committee in charge:

Professor Richard Norris, Chair
Professor Katherine Barbeau, Co-Chair
Professor Peter Franks

2024

The thesis of Zev Brook is approved, and it is acceptable in quality and form for publication on microfilm and electronically.

University of California San Diego

2024

TABLE OF CONTENTS

LIST OF FIGURES

LIST OF TABLES

ABSTRACT OF THE THESIS

High Open-Ocean Productivity in a Greenhouse World

by

Zev Brook

Master of Science in Oceanography

University of California San Diego 2024

Professor Richard Norris, Chair

The globally-warm climate of the Early Eocene Climatic Optimum (EECO) offers a potential analog for a future greenhouse world. Studying the Eocene ocean gives us a window into an Earth where marine carbon cycling may have been much different from what is observed in the present. I use a long barite record in the Indian Ocean to contrast carbon export between higher temperatures in the EECO and hyperthermal events with the comparatively cooler Middle Eocene. Barite accumulation rate serves as a proxy for export production due to the microenvironments in which it forms. I find that reconstructed export production went from a normal baseline to a peak in the hotter Early Eocene, implying a highly productive open ocean. The low abundance of organic carbon in the sedimentary record suggests that the Eocene ocean had almost complete remineralization.

BODY OF THE THESIS

We know from first principles (the Arrhenius equation) that chemical reactions run faster at higher temperatures, which includes both photosynthesis and respiration. Modeling work suggests that mean cell size and export production would have increased during the warm periods in Earth history like the Eocene epoch (Wilson et al. 2018). An exponential dependence is established for respiration on an individual level, with a noisier relationship on an ecosystem level (Yvon-Durocher et al. 2012). We would therefore expect that in hotter climates, marine ecosystems would look much different from those of today, with higher respiration and higher production accompanied by higher nutrient recycling than in the present ocean. Understanding how warm-climate ecosystems functioned can yield insight both into the past, as well as into potential future climate states.

The Early Eocene Climatic Optimum (EECO; about 54–49 Ma) was significantly and globally hotter than today, with tropical sea surface temperatures in the range of 30–36 °C and intense polar amplification (Evans et al. 2018). Deep water, formed at these hotter poles in the absence of polar ice, also had temperatures significantly higher than today, in the range of 5–12 °C (Cramer et al. 2011). The EECO, which was punctuated by transient warming events referred to as hyperthermals, represents a sustained warm state, the warmest on record in the past 90 million years (Zachos et al. 2008). The proximate cause of this warm state was high levels of atmospheric CO_2, around 1400 ppm (Anagnostou et al. 2016).

Deep-sea sediment cores dated to this interval are remarkably depauperate in organic matter (Thomas et al. 1992), which, on its face, seems inconsistent with high productivity. Yet evidence to support a productive pelagic ocean at various sites includes both previous studies on biogenic barite as well as other proxies, such as ichthyoliths, biomarker lipids, and benthic foraminiferal assemblages. In the open South Pacific, fish production as measured by ichthyolith accumulation rate is approximately six times higher during the EECO than in the early Paleocene (Sibert et al. 2016). This suggests that the disagreement between the organic matter record and other proxies reflects processes that occur during export, between production and burial.

Olivarez Lyle & Lyle 2006 detail a solution to this paradox which neatly explains both the biological and climatic characteristics of a warmer-than-modern ocean as part of a self-sustaining positive feedback loop. As respiration increases, shallow waters would become oxygen-depleted and regenerate phosphorus more easily (Sluijs et al. 2014). Increased rates of photosynthesis (with the commonly limiting phosphorus now supplied) would increase productivity even as increased rates of respiration would prevent carbon from accumulating on the seafloor, maintaining high atmospheric CO_2. Sharp $\delta^{13}C$ depth profiles of dissolved inorganic carbon (DIC) lend support to the idea of a shallow remineralization depth (John et al. 2014). Further compounding the positive feedback, this unfamiliar ocean would have many ecological disruptions to the biological pump, potentially including a rise in picophytoplankton dominance and a greater role for the upper-ocean microbial loop (Boscolo-Galazzo et al. 2018).

This work uses the deep-sea sediment barite record of Ocean Drilling Program (ODP) site 762 in the Indian Ocean to reconstruct the Eocene history of export production. Barite ($BaSO_4$, barium sulfate) is widely undersaturated in the ocean, but nevertheless regularly precipitates in microenvironments provided by the cell membranes of sinking organic matter, and the morphology of marine barite is consistent only with these microenvironments (Martinez-Ruiz et al. 2019; Light et al. 2023b). Once precipitated, barite is highly recalcitrant, and it is thought that as much as ~30% is incorporated into the sediment record (Dymond et al. 1992). Experimental work suggests that the barite which reaches the seafloor does so while still associated with organic matter, thus recording its export even if it is later respired (Light et al. 2023a). Contrary to the claims of Dickens et al. (2003), improved box modeling has shown that sustained high barite export to the seafloor does not have to deplete the marine barium pool and does not require an abiogenic source (Carter et al. 2020). Barite offers an elegant window onto an ecosystem-scale process, because although the mechanism of its precipitation remains debated, barite formation is not known to discriminate between the sources of organic matter flocs in which barite is crystallized. Despite these advantages, its use as a proxy has been limited by difficulties in measurement that arise from its low relative abundance and the need to exclude barite of terrestrial origin that has formed due to wholly unrelated factors before entering the ocean (Paytan et al. 1996). This study uses data collected through the method described in House and Norris (2020), which is a high-throughput, reproducible technique that sequentially dissolves barite.

The barite record discussed here was recovered from ODP Leg 122 Site 762 in the Exmouth Plateau of the Indian Ocean, off the northwest coast of Australia. The

site has been tectonically inactive and had little change in depth during the entire time period of interest (essentially, the Eocene epoch) until the present (Shamrock et al. 2012). The Indian Ocean is one of the less-studied ocean basins, and outside the anomalous, shallow Arabian Sea, the only work on Indian Ocean barite was a dated study that attempted to use it to measure plate velocity (Schmitz 1987). As a result, the present analysis provides potentially useful context with novel data for the ocean basin, at a site where barite has not been measured before, but stratigraphic work has been done.

The data used in this study were collected by B. House with the method described in House and Norris (2020). Previous methods correct for terrigenous barite by digesting everything and then applying a correction by means of a ratio with aluminum, which is assumed to be entirely terrigenous, or attempt to dissolve everything other than barite in a series of acid leaching steps. The first approach introduces significant and unpredictably inconsistent error depending on the composition of terrestrial silicates near the site, and the second consistently underestimates authigenic marine barite by dissolving some of it in the process. The House method avoids these pitfalls through dissolution of carbonates followed by dissolution of the barite itself. The sample is first completely dried, ground, and then treated with 4 N acetic acid to dissolve carbonates. Samples are washed and centrifuged before being leached with 0.2 M diethylenetriaminepentaacetic acid (DTPA) at a pH that maximizes Ba binding efficiency. The leachate can then be filtered and measured on an inductively coupled plasma–optical emission spectrometer (ICP–OES). For more details on the methods, and a description of the

tests that assured the reliability and reproducibility of the method, see House and Norris (2020).

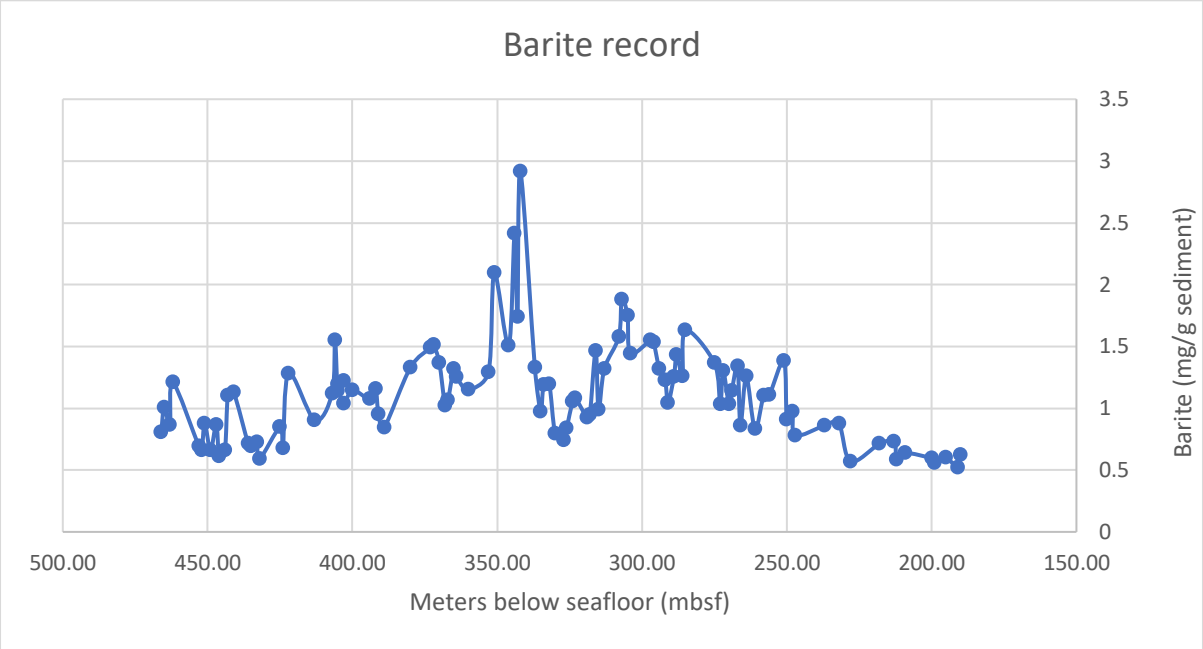

Figure 1: The measured barite record for Site 762 against depth in the sediment core.

A new age model was constructed for Site 762 to improve on existing work, including Shamrock et al. (2012), by using newer chronostratigraphic data and the updated geologic timescale of Gradstein (2012). First and last occurrence data for calcareous nannofossils and foraminifera from Gradstein (2012) and Agnini et al. (2014) were used to improve the biostratigraphic dates. Astronomically calibrated carbon and oxygen isotope data from Site 1209 from Westerhold et al. (2020) were used to improve the magnetostratigraphic dates, for which four reversals could be used within the Eocene. For the carbon isotope excursion associated with the Paleocene-Eocene Thermal Maximum (PETM), the age of 56.01 Ma was used, as proposed by Zeebe & Lourens (2019). Although Westerhold et al. (2017) date the Eocene Thermal Maximum 2 (ETM2) at 54.05 Ma, it was excluded as an event due to concerns about how definitively it could be identified in this particular record. For

the final age model, a revised version with only the best dates was produced, which used the aforementioned 4 magnetic reversals, the PETM, and 16 biostratigraphic events involving 14 microfossil species.

Table 1: Chronology datums used to produce the revised chronostratigraphy. References are as follows: W = Westerhold et al. (2020), G = Gradstein et al. (2012), A = Agnini et al. (2014), ZL = Zeebe & Lourens (2019).

Datum	Depth (MBSF)	Midpt.	Age (Ma)	Ref.
C17r/C18n	248.80–249.41	249.11	38.42	W
C22n/C22r	327.60–328.50	328.05	49.71	W
C24n/C24r	394.40–394.76	394.58	53.90	W
C24r/C25n	421.98–422.94	422.46	57.07	W
PETM	412.65	412.65	56.01	ZL
T *Discoaster saipanensis*	192.50–193.00	192.75	34.44	G
T *Discoaster barbadiensis*	192.50–193.00	192.75	34.76	G
T *Chiasmolithus grandis*	236.96–246.50	241.73	37.98	G
T *Chiasmolithus solitus*	268.50–269.25	268.88	40.40	G
B *Reticulofenestra reticulata*	276.71–284.05	280.38	41.66	G
T *Nannotetrina fulgens*	290.50–291.15	290.83	42.87	G
T *Chiasmolithus gigas*	291.15–292.00	291.58	44.12	G
B *Chiasmolithus gigas*	296.98–303.48	300.23	45.49	G
B *Blackites inflatus*	319.98–322.50	321.24	47.84	G
T *Tribrachiatus orthostylus*	332.75–333.52	333.14	50.50	G
B *Coccolithus crassus*	341.50–342.25	341.88	50.93	A
B *Discoaster lodoensis*	373.01–379.54	376.28	52.64	A (as Bc)
B *Tribrachiatus orthostylus*	394.93–398.30	396.62	54.37	G
B *Discoaster diastypus*	412.59–413.25	412.92	55.95	G
B *Rhomboaster bramlettei*	412.59–413.25	412.92	55.86	G
B *Discoaster multiradiatus*	422.00	422.00	57.21	G

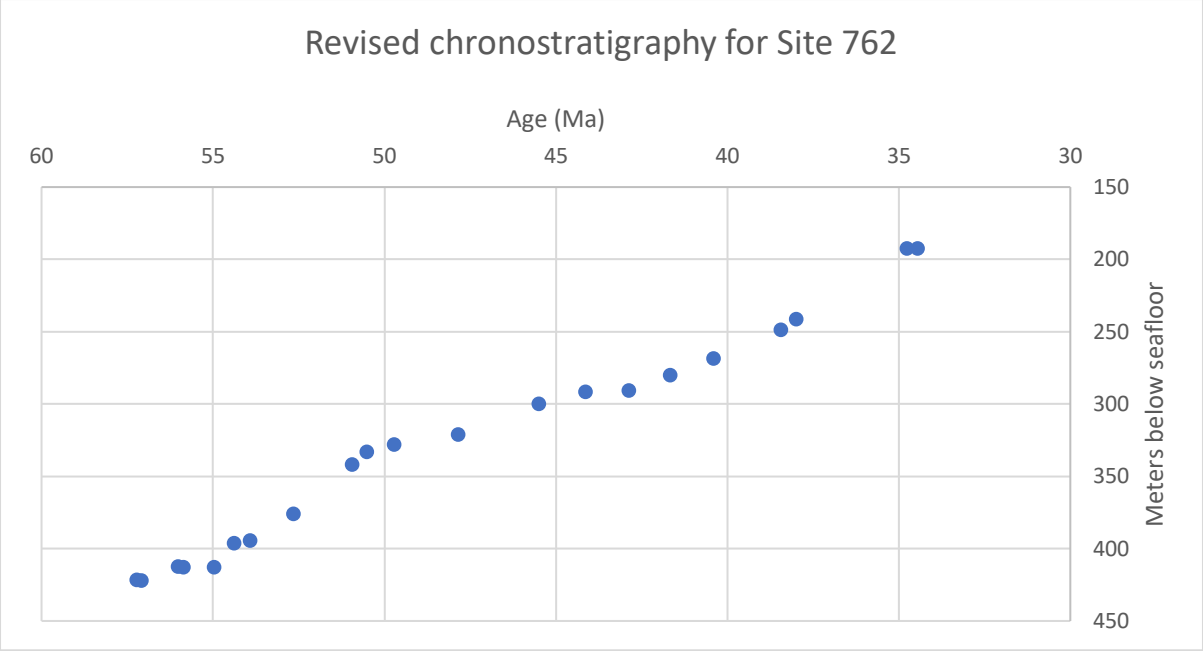

Figure 2: The revised chronostratigraphy for Site 762 based on the data in Table 1.

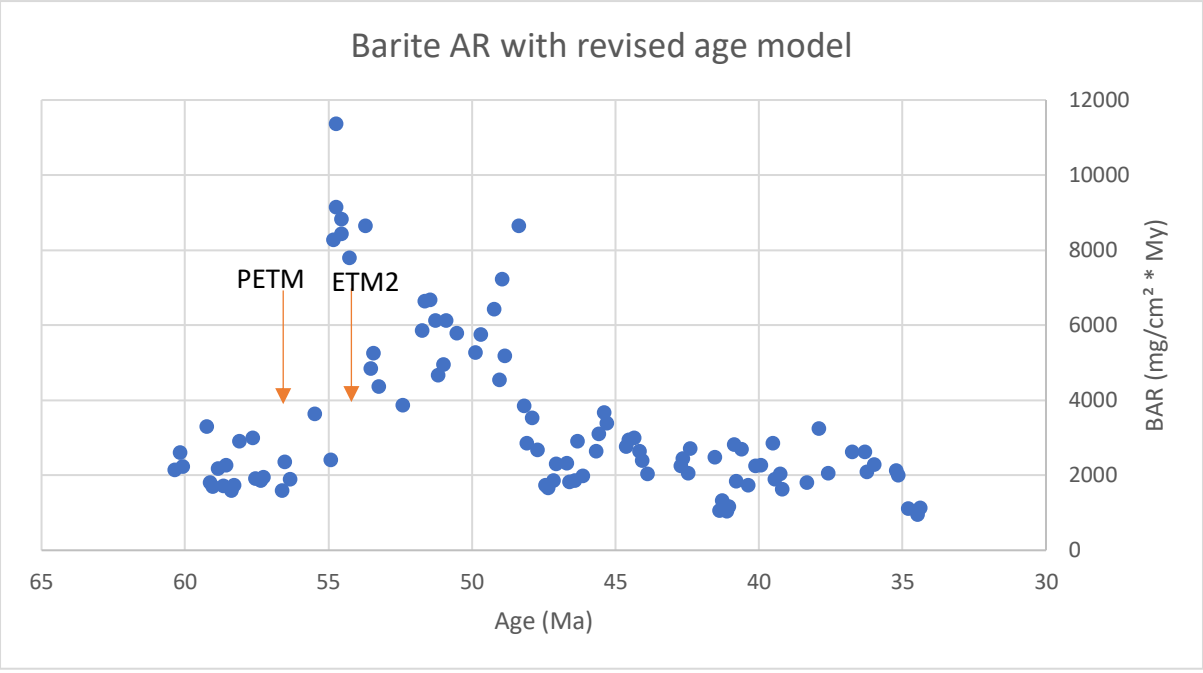

Figure 3: Barite accumulation rate for Site 762 using the revised age model and the sedimentation rates estimated by Shamrock et al. (2012).

The current latitude of Site 762 is 19.88˚S, but the Australian plate has moved north significantly during the Cenozoic (Scotese 2001), which has implications for

our expectations of productivity. Using a paleolatitude calculator with the paleomagnetic reference frame of Vaes et al. (2023), the latitude of this site 50 million years ago was approximately 40.78˚S (van Hinsbergen et al. 2015). In the context of the modern Indian Ocean, this difference would lie between the site's current location in the northern part of the subtropical zone and a paleolocation that would currently be in the northern part of the temperate zone. The barite record analyzed here ranges in age from about 60 to 34 Ma, during which time the site traveled northward about 6 degrees of latitude (van Hinsbergen et al. 2015). Although this change in latitude is not significant enough to render this analysis invalid, it would likely have some effect on productivity.

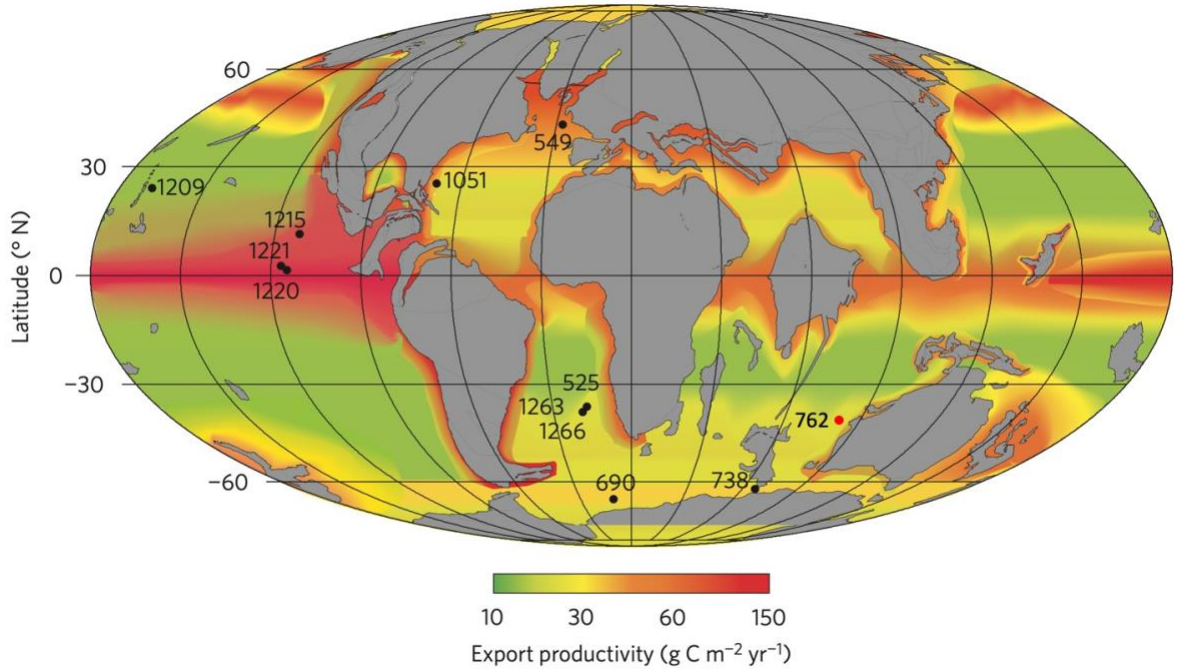

Figure 4: Figure 1b from Ma et al. (2014) showing model results for global export productivity at the height of the PETM with the approximate paleolocation of site 762 added in red.

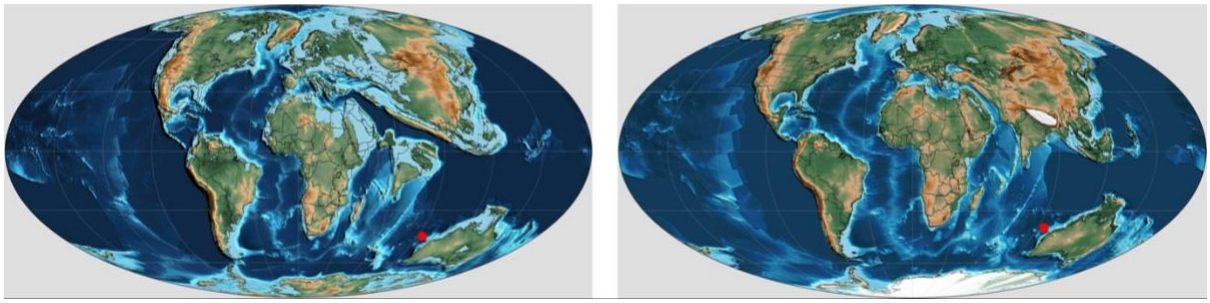

Figure 5: Maps from Scotese (2021)'s paleogeographic reconstruction for 55 Ma (left) and 35 Ma (right) with the approximate paleolocation of site 762 added in red.

New production was calculated using the equation from Ma et al. (2014). Ma et al.'s (2014) calculation of new production is based on the global core-top calibration study of Eagle et al. (2003). The method in Dymond et al. (1992) was considered superseded and not used. These linear equations based on core-top calibrations are considered more germane to deep-time sediment core data than the nonlinear equations based on sediment trap data (Carter et al. 2020). Unfortunately, the Eagle et al. (2003) equations were not published, and they used both published and unpublished data to build regression lines. Extracting the equation of the line from their Figure 4b yields $y = 1.44x + 13.2$ where x is the accumulation rate of barium in barite (mg/(m² * yr)) and y is carbon export (g C/(m² * yr)).[1] This matches well with the equation that Ma et al. (2014) use, which is $y = 1.462x + 12.821$, and the differences may plausibly be explained by different use of unpublished data belonging to A. Paytan. It may also be solely due to the exclusion of the single outlier in Eagle et al. (2003), a sample from the Peru margin (W7706) that shows anomalously high carbon export at low BAR and thus which, if removed, would cause the observed decrease in the y-intercept and slight increase in the slope.

[1] Note that the labels on Figure 4 in Eagle et al. (2003) erroneously say µg when mg is intended; this was amended in a correction published in the same journal.

Given the triviality of the differences, the equation from Ma et al. (2014) was used, which also corrects the dimensional analysis for their units[2], and multiplies by 58.8%, the portion of barite that is Ba by mass.

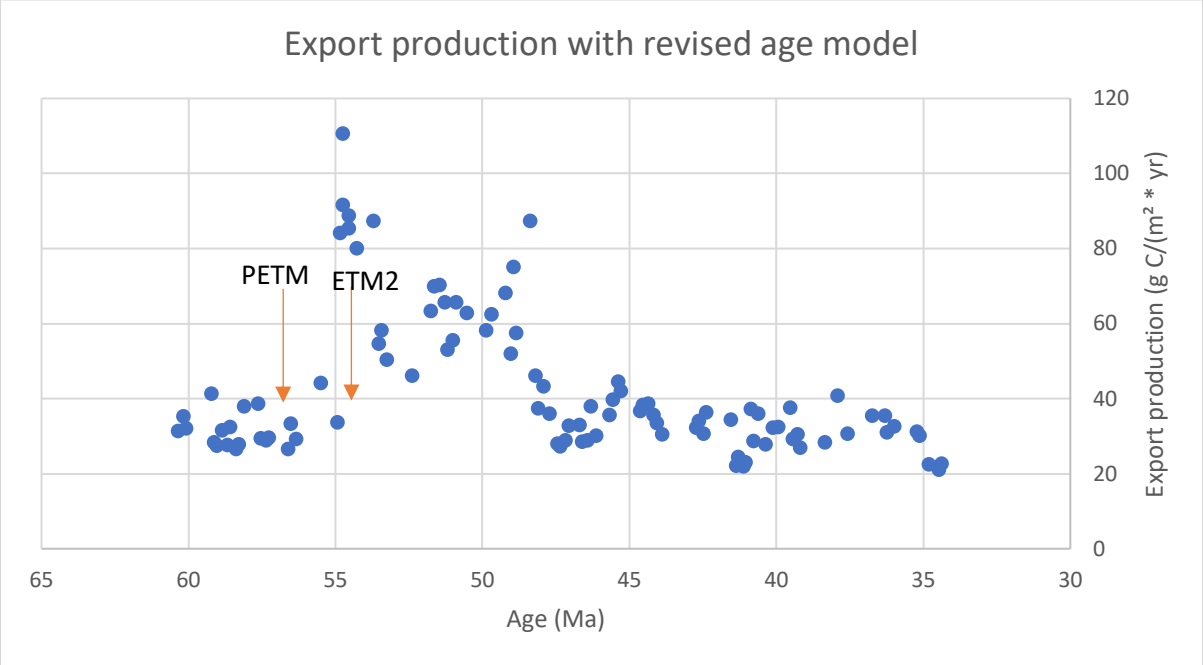

Figure 6: Estimated export production for Site 762 using the revised age model, the sedimentation rates estimated by Shamrock et al. (2012), and the equations of Ma et al. (2014).

The values for export production rise from a Paleocene value of ~30 g C/(m² * yr) to a peak of ~60–70 g C/(m² * yr) in the EECO and then settle back to the ~30 g C/(m² * yr) baseline around 48 Ma. On top of this broad pattern, there is a spike of very high values of about 90 ±20 g C/(m² * yr) during the major hyperthermal events (approximately 54.8 to 53.7 Ma), and potentially another more ambiguous spike around 49.2 to 48.4 Ma, although there are only three data points to support it. The

[2] Oddly, the equation used in their supplement also multiplies the entire expression by 10 and 0.1, which of course has no effect.

baseline values for the late Paleocene match the model prediction of Ma et al. (2014) as seen in Figure 3, but given that the figure is supposed to represent a time of BAR maxima, it would seem to heavily underestimate export production in the Indian Ocean. The most parsimonious reading of the time series is that there are essentially two states for production: a baseline state in the Paleocene and Middle Eocene, and a period during the EECO where export production is about twice that of the baseline, with the EECO state also being prone to potential spikes of geologically short duration.

In general, these baseline values are unsurprising for the site's latitude and similar to expectations for the modern ocean, with the notable exception of the EECO hump. The baseline sits around 20–40 g C/(m^2 * yr), which is right within expectations for its paleolatitude and ocean basin based on global estimates drawn from net primary productivity measurements in the modern (Falkowski et al. 1998). The post-EECO baseline may be slightly lower than the pre-EECO baseline, which could be explained by the northward drift of the site, but the data are noisy enough that such an explanation is not required. The unsurprising values start to seem more unusual in the context of an ocean that was still warmer and less oxygenated than it is today, although not to the same extent as the EECO. The EECO itself sits around 50–70 g C/(m^2 * yr), and the spikes, which reach a maximum value of 110.5 g C/(m^2 * yr) between the PETM and ETM, are considerably out of the range for such a site in the modern ocean, and resemble a coastal upwelling zone like the modern coast of Peru.

In order to discuss not just export production but total primary production, the f-ratio of site 762 in the Eocene would have to be estimated. The f-ratio, which measures the fraction of primary production fueled by nitrate (and therefore largely

derived from the aphotic zone), is considered to represent the relationship between primary production and new production that can be exported. Prakash et al. (2015) find widely varying f-ratios across the Indian Ocean, with significant variability in the tropical zone (0.13–0.45) and a mean of 0.50 in the southern Indian Ocean. Informed by the paleolatitude estimate, 0.50 appears to be a reasonable value for the f-ratio, thus matching the value used for the Southern Ocean in Eagle et al. (2003), who did not look at any sites in the Indian Ocean. However, the f-ratio has dependence on temperature, and much lower values would be expected in a hotter climate (Laws et al. 2000). As a result, any reconstruction of primary production in surface waters is ill-advised, because it is likely that the f-ratio itself changed during the time of interest, and it cannot be meaningfully modeled.

The carbon export and productivity estimates produced for this site can only be considered on a qualitative, rather than a quantitative level, because it is problematic to assume that barite preservation rate necessarily remained constant. Just like prior work using this proxy, it is possible that changes in the dissolution and preservation of barite both as it sinks in the water column and in the sediments are being misinterpreted as changes in production of barite (Carter et al. 2020), despite the fact that there is no *a priori* reason to believe there was any such change at this site. Various other sources of error include minor instrumental error, minor error that remains in the extraction method, error in the linear equation used to estimate production, and error in the chronology (which could be ameliorated with a higher-resolution C isotope record) and sedimentation rate estimates. In particular, a simplistic (mostly static) sedimentation rate would partially or wholly eliminate the spike at the hyperthermals and show a more subdued hump that peaks slightly later. There is also methodological reason to believe that studies like Eagle et al. (2003)

systematically underestimated marine barite by dissolving some of it in their extraction process (House and Norris 2020), in which case the more effective House method might in fact overestimate production and require recalibration of the production equation. However, the scale of the changes observed in reconstructed carbon export, where the export production in the EECO is around three times the Paleocene and Middle Eocene values, suggest that the signal observed is real. Although there is no guarantee that the values themselves are meaningful, they are reasonable and can easily be refined by future work.

Given the signal in the barite record, why isn't there any associated trend in the organic matter record? Two factors could act to prevent all this exported organic matter from being buried. Firstly, the increase in respiration rates likely would have exceeded the increase in photosynthetic rates. Secondly, the community composition of the phytoplankton themselves could change, producing a more labile pool of carbon that could be consumed before sinking as deep. This would entail highly productive shallow waters and hypoxic midwaters, where nutrients stay near the surface and are recycled vigorously, and the oxygen minimum zone expands.

To the extent that these hypotheses involve organic matter that never in fact makes it to the seafloor, this may not be consistent with the idea that barite dissolution may be preferential and that the barite proxy in fact measures the arrival of organic matter to the seafloor rather than its export (Light et al. 2023b). This implies a somewhat different scenario: increased regeneration leads to increased production in surface waters, but sinking organic matter travels through hypoxic midwaters to the seafloor. This labile organic carbon would then be remineralized by the benthic community, and benthic waters would be saturated with respect to barite,

allowing the barite that had traveled with the organic matter to be buried and incorporated into the sedimentary record.

Given ongoing anthropogenic warming, it would be reasonable to compare these results with model outputs for the near future. Unfortunately, there is no consensus on how to model the carbon pump's response to warming, with a wide range of estimates in export production from –41% to +1.8% (Henson et al. 2022). Most model outputs predict a decrease in export production, which would seem to disagree with the findings discussed above. During the EECO, export production increased, and even the record before and after the EECO is reconstructed to have been warmer than the modern (Westerhold et al. 2020), yet shows export production that agrees with modern expectations. However, the dynamics involved likely differ significantly between a geologically instantaneous warming event, like the one we are currently experiencing, and the Eocene's prolonged, steady-state warm period. The Eocene hyperthermal events, which were geologically rapid but not instantaneous warming events, have been considered a natural analog to anthropogenic warming. They show even starker increases in export production, although we still cannot exclude the possibility that they may have perturbed the marine carbon cycle in a fundamentally different manner. Additionally, these global model results may, even if correct, paper over significantly different outcomes in different latitudes and ocean basins; the results here should not be expected to agree with, for example, findings of decreased productivity in the tropics during the same time (Moretti et al. 2024).

As the most recent period of sustained warmth in Earth history, the EECO provides not only a potential analog to the future oceans, but also helps us understand how the marine biosphere functions in alien conditions. This work

advances that effort using a record from an understudied ocean basin, and finds that carbon export from the open ocean to the seafloor increased significantly during the EECO. I have shown that at a site in the Indian Ocean, a somewhat hotter climate had export that was unremarkable from a modern perspective, and a much hotter climate saw a dramatic increase in export.

REFERENCES

Agnini, C., Fornaciari, E., Raffi, I., Catanzariti, R., Pälike, H., Backman, J., & Rio, D. (2014). Biozonation and biochronology of Paleogene calcareous nannofossils from low and middle latitudes. *Newsletters on Stratigraphy*, *47*(2), 131–181. https://doi.org/10.1127/0078-0421/2014/0042

Anagnostou, E., John, E. H., Edgar, K. M., Foster, G. L., Ridgwell, A., Inglis, G. N., Pancost, R. D., Lunt, D. J., & Pearson, P. N. (2016). Changing atmospheric CO2 concentration was the primary driver of early Cenozoic climate. *Nature*, *533*(7603), 380–384. https://doi.org/10.1038/nature17423

Boscolo-Galazzo, F., Crichton, K. A., Barker, S., & Pearson, P. N. (2018). Temperature dependency of metabolic rates in the upper ocean: A positive feedback to global climate change? *Global and Planetary Change*, *170*, 201–212. https://doi.org/10.1016/j.gloplacha.2018.08.017

Carter, S. C., Paytan, A., & Griffith, E. M. (2020). Toward an improved understanding of the marine barium cycle and the application of marine barite as a paleoproductivity proxy. *Minerals*, *10*(5), 421. https://doi.org/10.3390/min10050421

Cramer, B. S., Miller, K. G., Barrett, P. J., & Wright, J. D. (2011). Late Cretaceous–Neogene trends in deep ocean temperature and continental ice volume: reconciling records of benthic foraminiferal geochemistry (δ18O and Mg/Ca) with sea level history. *Journal of Geophysical Research*, *116*(C12). https://doi.org/10.1029/2011jc007255

Dickens, G. R., Fewless, T., Thomas, E., & Bralower, T. J. (2003). Excess barite accumulation during the Paleocene-Eocene Thermal Maximum: Massive input of dissolved barium from seafloor gas hydrate reservoirs. In Wing, S. L., Gingerich, P. D., Schmitz, B., and Thomas, E. (eds.), Causes and Consequences of Globally Warm Climates in the early Paleogene, Geological Society of America Special Paper 369, 11–23.

Dymond, J., Suess, E., & Lyle, M. (1992). Barium in deep-sea sediment: A geochemical proxy for paleoproductivity. *Paleoceanography*, *7*(2), 163–181. https://doi.org/10.1029/92pa00181

Eagle, M., Paytan, A., Arrigo, K. R., van Dijken, G., & Murray, R. W. (2003). A comparison between excess barium and barite as indicators of carbon export. *Paleoceanography*, *18*(1). https://doi.org/10.1029/2002pa000793

Evans, D., Sagoo, N., Renema, W., Cotton, L. J., Müller, W., Todd, J. A., Saraswati, P. K., Stassen, P., Ziegler, M., Pearson, P. N., Valdes, P. J., & Affek, H. P. (2018). Eocene greenhouse climate revealed by coupled clumped isotope-mg/ca thermometry. *Proceedings of the National Academy of Sciences*, *115*(6), 1174–1179. https://doi.org/10.1073/pnas.1714744115

Falkowski, P. G., Barber, R. T. & Smetacek, V. (1998). Biogeochemical controls and feedbacks on open ocean production. *Science*, *281(5374)*, 200–206.

Gradstein, F. M. (2012). *The Geologic Time Scale 2012*. Elsevier.

Henson, S. A., Laufkötter, C., Leung, S., Giering, S. L. C., Palevsky, H. I., & Cavan, E. L. (2022). Uncertain response of ocean biological carbon export in a changing world. *Nature Geoscience*, *15*, 248–254.

House, B. M., & Norris, R. D. (2020). Unlocking the barite paleoproductivity proxy: A new high-throughput method for quantifying barite in marine sediments. *Chemical Geology*, *552*, 119664. https://doi.org/10.1016/j.chemgeo.2020.119664

John, E. H., Wilson, J. D., Pearson, P. N., & Ridgwell, A. (2014). Temperature-dependent remineralization and carbon cycling in the warm Eocene oceans. *Palaeogeography, Palaeoclimatology, Palaeoecology*, *413*, 158–166. https://doi.org/10.1016/j.palaeo.2014.05.019

Laws, E. A., Falkowski, P. G., Smith, W. O., Ducklow, H., & McCarthy, J. J. (2000). Temperature effects on export production in the open ocean. *Global Biogeochemical Cycles, 14(4)*, 1231–1246.

Light, T., Garcia, M., Prairie, J. C., Martínez-Ruiz, F., & Norris, R. (2023a). Water column barium sulfate dissolution and shielding by organic matter aggregates: Implications for the pelagic barite proxy. *Chemical Geology*, *636*, 121637. https://doi.org/10.1016/j.chemgeo.2023.121637

Light, T., Martínez-Ruiz, F., & Norris, R. (2023b). Marine barite morphology as an indicator of biogeochemical conditions within organic matter aggregates. *Geochimica et Cosmochimica Acta*, *358*, 38–48. https://doi.org/10.1016/j.gca.2023.08.012

Ma, Z., Gray, E., Thomas, E., Murphy, B., Zachos, J., & Paytan, A. (2014). Carbon sequestration during the Palaeocene–Eocene Thermal Maximum by an efficient biological pump. *Nature Geoscience*, *7*(5), 382–388. https://doi.org/10.1038/ngeo2139

Martinez-Ruiz, F., Paytan, A., Gonzalez-Muñoz, M. T., Jroundi, F., Abad, M. M., Lam, P. J., Bishop, J. K. B., Horner, T. J., Morton, P. L., & Kastner, M. (2019). Barite formation in the ocean: Origin of amorphous and crystalline precipitates. *Chemical Geology*, *511*, 441–451. https://doi.org/10.1016/j.chemgeo.2018.09.011

Moretti, S., Auderset, A., Deutsch, C., Schmitz, R., Gerber, L., Thomas, E., Luciani, V., Petrizzo, M. R., Schiebel, R., Tripati, A., Sexton, P., Norris, R., D'Onofrio, R., Zachos, J., Sigman, D. M., Haug, G. H., & Martínez-García, A. (2024). Oxygen rise in the tropical upper ocean during the Paleocene-Eocene thermal maximum. *Science*, *383*(6684), 727–731. https://doi.org/10.1126/science.adh4893

Olivarez Lyle, A., & Lyle, M. W. (2006). Missing organic carbon in Eocene marine sediments: is metabolism the biological feedback that maintains end-member climates? *Paleoceanography*, *21*(2). https://doi.org/10.1029/2005pa001230

Paytan, A., Kastner, M., & Chavez, F. P. (1996). Glacial to interglacial fluctuations in productivity in the equatorial Pacific as indicated by marine barite. *Science*, *274*(5291), 1355–1357. https://doi.org/10.1126/science.274.5291.1355

Prakash, S., Ramesh, R., Sheshshayee, M. S., Mohan, R., & Sudhakar, M. (2015). Nitrogen uptake rates and f-ratios in the Equatorial and Southern Indian Ocean. *Current Science*, *108*(2), 239–245.

Schmitz, B. (1987). Barium, equatorial high productivity, and the northward wandering of the Indian continent. *Paleoceanography*, *2*(1), 63–77. https://doi.org/10.1029/pa002i001p00063

Scotese, C. R. (2001). *Atlas of Earth History*. University of Texas at Arlington Department of Geology. PALEOMAP Project.

Scotese, C. R. (2021). An Atlas of Phanerozoic Paleogeographic Maps: The Seas Come In and the Seas Go Out. *Annual Review of Earth and Planetary Sciences*, *49*, 679–728.

Shamrock, J. L., Watkins, D. K., & Johnston, K. W. (2012). Eocene biogeochronology and magnetostratigraphic revision of ODP Hole 762C, Exmouth Plateau (northwest Australian Shelf). *Stratigraphy*, *9*(1), 55–75.

Sibert, E. C. (2016). Ichthyoliths as a paleoceanographic and paleoecological proxy and the response of open ocean fish to Cretaceous and Cenozoic global change. PhD thesis, https://escholarship.org/content/qt60d8q1w2/qt60d8q1w2

Sluijs, A., van Roij, L., Harrington, G. J., Schouten, S., Sessa, J. A., LeVay, L. J., Reichart, G.-J., & Slomp, C. P. (2014). Warming, euxinia and sea level rise during the Paleocene–Eocene thermal maximum on the Gulf Coastal Plain: implications for ocean oxygenation and nutrient cycling. *Climate of the Past*, *10*(4), 1421–1439. https://doi.org/10.5194/cp-10-1421-2014

Thomas, E., Shackleton, N. J., & Hall, M. A. (1992). Data report: Carbon isotope stratigraphy of Paleogene bulk sediments, Hole 762C (Exmouth Plateau, Eastern Indian Ocean). *Proceedings of the Ocean Drilling Program, 122 Scientific Results*. https://doi.org/10.2973/odp.proc.sr.122.195.1992

Vaes, B., van Hinsbergen, D. J., van de Lagemaat, S. H. A., van der Wiel, E., Lom, N., Advokaat, E. L., Boschman, L. M., Gallo, L. C., Greve, A., Guilmette, C., Li, S., Lippert, P. C., Montheil, L., Qayyum, A. & Langereis, C. G. (2023). A global apparent polar wander path for the last 320 Ma calculated from site-level paleomagnetic data. *Earth-Science Reviews, 245(104567).*

van Hinsbergen, D. J., de Groot, L. V., van Schaik, S. J., Spakman, W., Bijl, P. K., Sluijs, A., Langereis, C. G., & Brinkhuis, H. (2015). A paleolatitude calculator

for paleoclimate studies. *PLOS ONE*, *10*(6). https://doi.org/10.1371/journal.pone.0126946

Westerhold, T., Marwan, N., Drury, A. J., Liebrand, D., Agnini, C., Anagnostou, E., Barnet, J. S., Bohaty, S. M., De Vleeschouwer, D., Florindo, F., Frederichs, T., Hodell, D. A., Holbourn, A. E., Kroon, D., Lauretano, V., Littler, K., Lourens, L. J., Lyle, M., Pälike, H., Röhl, U., Tian, J., Wilkens, R., Wilson, P., & Zachos, J. C. (2020). An astronomically dated record of Earth's climate and its predictability over the last 66 million years. *Science*, *369*(6509), 1383–1387. https://doi.org/10.1126/science.aba6853

Wilson, J. D., Monteiro, F. M., Schmidt, D. N., Ward, B. A., & Ridgwell, A. (2018). Linking marine plankton ecosystems and climate: a new modeling approach to the warm early Eocene climate. *Paleoceanography and Paleoclimatology*, *33*(12), 1439–1452. https://doi.org/10.1029/2018pa003374

Yvon-Durocher, G., Caffrey, J. M., Cescatti, A., Dossena, M., Giorgio, P. del, Gasol, J. M., Montoya, J. M., Pumpanen, J., Staehr, P. A., Trimmer, M., Woodward, G., & Allen, A. P. (2012). Reconciling the temperature dependence of respiration across timescales and ecosystem types. *Nature*, *487*(7408), 472–476. https://doi.org/10.1038/nature11205

Zachos, J. C., Dickens, G. R., & Zeebe, R. E. (2008). An early Cenozoic perspective on greenhouse warming and carbon-cycle dynamics. *Nature*, *451*(7176), 279–283. https://doi.org/10.1038/nature06588

Zeebe, R. E., & Lourens, L. J. (2019). Solar system chaos and the Paleocene–Eocene boundary age constrained by geology and astronomy. *Science*, *365*(6456), 926–929. https://doi.org/10.1126/science.aax0612